Visualising Feasible Operating Ranges within Tissue Engineering Systems Using a "Windows of Operation" Approach: A Perfusion-Scaffold Bioreactor Case Study.

Ryan J. McCoy, Eng.D[1,2]

Tel.: +353 1 402 8508;
E-mail address: ryanmccoy@rcsi.ie

Fergal J. O'Brien, Ph.D[1,2] (Corresponding Author)

Tel.: +353 1 402 2149;
fax: +353 1 402 2355.
E-mail address: fjobrien@rcsi.ie

1. Department of Anatomy
   Royal College of Surgeons in Ireland
   123 St. Stephen's Green
   Dublin 2
   Ireland

2. Trinity Centre for Bioengineering,
   Trinity College Dublin,
   Dublin,
   Ireland

Short Running Title: Windows of operation in tissue engineering

Abstract

Tissue engineering approaches to developing functional substitutes are often highly complex, multivariate systems where many aspects of the biomaterials, bio-regulatory factors or cell sources may be controlled in an effort to enhance tissue formation. Furthermore, success is based on multiple performance criteria reflecting both the quantity and quality of the tissue produced. Managing the trade-offs between different performance criteria is a challenge. A "windows of operation" tool that graphically represents feasible operating spaces to achieve user-defined levels of performance has previously been described by researchers in the bio-processing industry. This paper demonstrates the value of "windows of operation" to the tissue engineering field using a perfusion-scaffold bioreactor system as a case study. In our laboratory, perfusion bioreactor systems are utilised in the context of bone tissue engineering to enhance the osteogenic differentiation of cell-seeded scaffolds. A key challenge of such perfusion bioreactor systems is to maximise the induction of osteogenesis but minimise cell detachment from the scaffold. Two key operating variables that influence these performance criteria are the mean scaffold pore size and flow-rate. Using cyclooxygenase-2 and osteopontin gene expression levels as surrogate indicators of osteogenesis, we employed the "windows of operation" methodology to rapidly identify feasible operating ranges for the mean scaffold pore size and flow-rate that achieved user-defined levels of performance for cell detachment and differentiation. Incorporation of such tools into the tissue engineer's armoury will hopefully yield a greater understanding of the highly complex systems used and help aid decision making in future translation of products from the bench top to the market place.

Key words: Tissue Engineering, Windows of Operation, Perfusion bioreactor, Collagen Scaffolds

Introduction

Tissue engineering is “an interdisciplinary field that applies the principles of engineering and life sciences toward the development of biological substitutes that restore, maintain, or improve tissue function or a whole organ" (Langer and Vacanti, 1993). The methods utilised are often highly complex, multivariate procedures, where many aspects of the biomaterials (e.g. composition, stiffness, and degradation rates), bio-regulatory factors (e.g. chemical reagents, mechanical stimuli) or cell sources may be controlled in an effort to enhance tissue formation. The choices made with respect to these input (independent) variables will ultimately determine the type, quality and quantity of tissue produced, which is typically assessed as a function of numerous output (dependent) variables or performance endpoints (e.g. cell viability and gene/protein expression level). Thus a major challenge for researchers concerns determining the optimal operating conditions that will yield the desired levels of tissue performance or functioning. Furthermore, it is also important to understand the feasibility and ease with which these specifications can be met; where the boundaries of the operating ranges lie that yield the desired levels of tissue performance or functioning.

“Windows of operation” plots are two-dimensional maps showing regions of feasible operating ranges for input variables after applying user defined constraints indicative of a required level of performance or functioning for measurable output variables. The construction of such two-dimensional maps has previously been described by researchers in the bio-processing industries where they were applied in the optimisation of large scale protein/antibody manufacturing processes (Salte et al., 2006; Woodley and Titchener-Hooker, 1996; Zhou and Titchener-Hooker, 1999). For example, the performance levels of different centrifuge types were assessed with respect to their clarification, dewatering and product yield capabilities based on the limits of their individual operating capacities (Salte et al., 2006). In addition to rapidly deducing feasible operating regions, the strength of these

graphical visualisation methods lies in their ability to gain greater understanding regarding the influence of key operating variables on the overall system behaviour.

The purpose of this paper is to firstly introduce the windows of operation concept to the tissue engineering community and secondly, using a perfusion bioreactor case study, to show how it may be conceptually applied to a specific problem. In our laboratory, perfusion bioreactor systems are utilised in the context of bone tissue engineering whereby highly porous cell-seeded collagen glycoaminoglycan (GAG) scaffolds are perfused with media to mechanically stimulate cells and thereby enhance osteogenic differentiation (Jaasma and O'Brien, 2008; Keogh et al., 2011; Partap et al., 2009; Plunkett et al., 2010). This perfusion-scaffold bioreactor system has been used as a model to illustrate the formulation, development and application of "windows of operation". Two key variables of perfusion-scaffold systems are the mean scaffold pore size and the perfusion flow rate (mean shear stress), both of which have been shown to influence successful tissue engineering. Altering the mean pore size has been shown to influence initial cell attachment levels (Murphy et al., 2010; O'Brien et al., 2005) as well as the ratio of cell morphology attachment types (McCoy et al., 2012). In these highly porous scaffolds, cells can attach in one of two morphologies, flat (akin to 2D monolayer culture) or bridging (where the cell spans the void space of the pore) (Annaz et al., 2004; McCoy et al., 2012; McMahon, 2007). In scaffolds with very large mean pore sizes, cells are not capable of spanning across the void space and thus a flat morphology type dominates. As mean pore size decreases, the ease of spanning the void space increases, and thus the proportion of cells adapting a bridging morphology type increases. The relevance of cell attachment morphology type becomes important when flow perfusion is applied to the cell-seeded scaffold.

Flow perfusion creates shear stresses within the scaffold that are sensed by the cells. Translation of these physical forces to a biological signal is termed mechanotransduction,

with cytoskeletal deformation being one of the primary mechanisms. If a cell adapts a bridging morphology type it will undergo greater levels of cytoskeletal deformation than a flat cell when subjected to the same flow conditions (Jungreuthmayer et al., 2009) and therefore also experience a greater degree of mechanical stimulation and hence differentiation; the cell alignment to the direction of flow creates a greater level of resistance leading to a larger deformation, like a sail in the wind. However, when the physical forces acting on the cell exceed the adhesion strength of the cell, then instead of deforming the cell and causing mechanical stimulation resulting in cellular differentiation, the cell is detached from the scaffold. Therefore bridging cells are also more susceptible to cell detachment than flatly attached cells when subjected to the same flow conditions (McCoy et al., 2012). Thus a key challenge of such perfusion bioreactor systems is to maximise the induction of osteogenic differentiation but minimise cell detachment from the scaffold. Cell detachment commonly occurs in flow-perfusion culture strategies (Plunkett et al., 2010; McCoy et al., 2012; Cartmell, S. et al., 2003; Alvarez-Barreto and Sikavitsas, 2007; Alvarez-Barreto et al., 2007) and should be minimised as it is an undesirable artefact having multiple implications from economic (cell culture costs) and clinical efficacy (loss of cell to cell communication and loss of bioactivity) perspectives. Maximising the induction of cell differentiation is the fundamental purpose in any tissue engineered product derived from progenitor cells. Cell differentiation however is a complex phenomenon, temporal in nature, having numerous markers indicative of different maturation stages.

To demonstrate the application of “windows of operation”, the levels of cell detachment and cell differentiation were quantified for osteoblast seeded collagen GAG (CG) scaffolds with a range of mean pore sizes (85, 120 or 325μm) when subjected to mean shear stresses of 0.0009, 0.0176 and 0.0879Pa using a perfusion bioreactor system. Cell differentiation was measured using cyclooxygenase-2 (COX2) and osteopontin (OPN) gene expression levels,

which essentially act as surrogate indicators of osteogenesis. The "windows of operation" approach was then applied to these data to identify feasible operating ranges with respect to mean pore size and mean shear stress that allowed pre-defined performance levels for cell detachment and differentiation to be achieved.

Materials and Methods

Creating "Windows of Operation"

"Windows of operation" are constructed by initially representing data for a single output variable in the form of a contour plot. Contours plots allow 3D (x, y, z) data to be plotted in a 2D (x, y) format where the third dimension is represented as a series of contour lines where combinations of the input variables (x, y) have equal z values. In this study the axes x and y represent mean pore size (in the range of 85 - 325μm) and mean shear stress (in the range of 0 – 0.879Pa) respectively. The third dimension z is represented by either the percentage of cell detachment, the fold change in COX2 gene expression levels or the fold change in OPN gene expression levels. More specifically, each contour line can be considered as a function of two independent variables (mean pore size and mean shear stress) where the function has a constant output value (z) for the dependent variable, for example, 10% cell detachment. By overlaying multiple contour plots for different dependent variables, while keeping the independent variables ranges constant, overlapping regions can be viewed rapidly allowing the user to swiftly and easily identify operating ranges, "windows of operation", where both dependent variables are feasible. "Windows of operation" were created by constructing individual contour plots based on user defined constraints using SigmaPlot Version 11.2 (Systat Software Inc., CA, USA) and manually overlaying them prior to colouring the "window of operation" using Adobe Photoshop Elements 7.0 (Adobe Systems Incorporated, San Jose, CA, USA).

Scaffold Fabrication

Collagen GAG (CG) scaffolds were fabricated in accordance with a previously developed protocol (O'Brien et al., 2004). Briefly, a CG suspension was created by blending micro-fibrillar bovine tendon collagen (Integra Life Sciences, Plainsboro, NJ) with chondroitin-6-sulphate sodium salt, isolated form shark cartilage (Sigma-Aldrich, Dublin, Ireland) in 0.05M acetic acid (Fisher Scientific Loughborough, Leicestershire, UK), the CG suspension was degassed under vacuum and freeze-dried (Advantage EL, VirTis Co., Gardiner, NY). A final freezing temperature of -10^{o}C, -40^{o}C and -60^{o}C yielded mean pore sizes of 325, 120 and 85μm respectively. Post lyophilisation scaffold sheets were dehydrothermally cross-linked at 105^{o}C for 24h in a vacuum oven at 50mTorr (VacuCell, MMM, Germany).

Individual scaffold discs (diameter 12.7mm; depth 3-4mm) were punched out of the sheets and further strengthened through chemical cross-linking; scaffolds were submersed within an aqueous solution of 14mM N-(3-dimethylaminopropyl)-N0-ethylcarbodiimide hydrochloride (EDAC) (Sigma-Aldrich) and 5.5mM N-Hydroxysuccinimide (NHS) (Sigma-Aldrich) for 2h at room temperature before being washed and stored in PBS.

Bioreactor Experiments

The pre-osteoblastic cell line, MC3T3-E1 (<passage 30), was cultured in alpha-minimum essential media (α-MEM) (Sigma-Aldrich) supplemented with 10% foetal bovine serum (Biosera, East Sussex, UK), 1% L-glutamine (Sigma–Aldrich) and 2% penicillin/streptomycin (Sigma–Aldrich). The cells were maintained as sub-confluent monolayers in T175 flasks under standard conditions (37^{o}C, 5% CO_2). Cells were detached with Trypsin–EDTA (Sigma–Aldrich) and re-suspended at a concentration of $1x10^7$ cells/mL. Scaffolds (with mean pore sizes of either 85, 120 or 325 μm) were seeded with a total of

$2x10^6$ cells as previously described (McCoy et al., 2012) and pre-cultured statically for 6 days (media change on day 3). Seeded scaffolds were then either cultured statically or exposed to a steady state fluid flow regime (0.05, 1 or 5mL/min equating to 0.0009, 0.0176 and 0.0879Pa respectively (McCoy et al., 2012)) in the perfusion bioreactor for 48h; conditions that have been previously shown to enhance osteogenesis of MC3T3 cell-seeded scaffolds by our group, but resulted in cell detachment of up to 40% (Jaasma and O'Brien, 2008). During bioreactor culture, six constructs were cultured simultaneously, but each had a separate syringe scaffold chamber reservoir system. Given that the bioreactor system does not form a looped fluid circuit, the syringe requires re-filling to maintain continuous flow through the construct. Thus, the direction of medium flow through the bioreactor system was reversed periodically; every 300 min for 0.05mL/min, every 15 min for 1mL/min and every 3 min for 5mL/min. Constructs for the static culture group were transferred to a new 6-well plate and cultured in 5mL of fresh medium. Post-culture constructs were flash frozen in liquid nitrogen and stored at -80^{o}C until analysis.

Quantification of Cell Detachment

DNA was isolated from the constructs by homogenisation in RLT lysis buffer (Qiagen, Crawley West Sussex, UK) supplemented with β-mercaptoethanol (1%v/v) (Sigma-Aldrich) in a rotor-stator homogeniser (Omni International, Kennesaw, GA, USA). Cell lysates were centrifuged using QI Shredder columns (Qiagen) and the resulting supernatant stored at -80^{0}C. DNA quantification was performed using a Quant-iT™ PicoGreen dsDNA kit (Invitrogen, Bio-sciences, Dublin, Ireland) in accordance with manufacturer's instructions. Fluorescence of the samples was measured (excitation 480nm, emission 538nm) using a fluorescent plate reader (Varioskan Flash 100-240V, Thermo Scientific) and DNA concentration was deduced using a standard curve. DNA concentrations at 48h were normalised to a 0hr control to determine the levels of cell detachment.

Quantification of COX2and OPN Gene Expression

COX2 and OPN gene expression levels were chosen for quantification as they have been previously shown to be significantly up-regulated in our laboratory by osteoblast seeded collagen GAG scaffolds in response to perfusion bioreactor culture (Jaasma and O'Brien, 2008; Partap et al., 2009). Furthermore, COX2 is a key osteogenic marker that has been studied extensively in the literature and shown to be up-regulated significantly in response to mechanical stimulation during the early stages of mechanically induced osteogenesis (Forwood, 1996; Klein-Nulend et al., 1997; Wadhwa et al., 2002a; Wadhwa et al., 2002b). COX2 plays a key role in the production of prostaglandin E2 (PGE2), which is critical for bone formation and furthermore, COX2 knockout mice have been shown to exhibit decreased mesenchymal progenitor cell differentiation into osteoblasts (Zhang et al., 2002). OPN is also typically expressed during the early stages of osteogenic differentiation and is believed to play a significant role in bone remodelling through aiding the attachment of osteoclasts (bone reabsorbing cells) to the bone matrix.

RNA was extracted from the supernatants harvested during DNA extraction using an RNeasy mini kit (Qiagen) according to manufacturer instructions. The quality and concentration of RNA was quantified by measuring absorbance at 260nm (GeneQuant Pro RNA/DNA calculator, Biochrom Ltd., UK). Reverse transcription was performed on 400ng of total RNA using the QuantiTect RT Kit (Qiagen) according to the manufacturer's instructions on an Eppendorf thermal cycler (Mastercycler Personal, Eppendorf, Cambridge, UK). RT–PCR was subsequently performed using a 7500 Real-Time PCR System (Applied Biosystems, Foster City, CA) using the QuantiTect SYBR Green PCR Kit (Qiagen) according to the manufacturer's instructions with Quanti-Tect Primers designed by Qiagen. Results were quantified for COX2 (NM_017232) and OPN (NM_012881) via the relative quantification ($\Delta\Delta$Ct) method (Livak and Schmittgen, 2001) using 18-S rRNA (M11188) as the endogenous

reference. For each gene, results are expressed relative to a 0h control group. All PCR reactions were conducted in duplicate for each sample.

Statistics

Statistical analysis was conducted using a two-way ANOVA followed by a post hoc Holm-Sidak test for pairwise comparisons using Sigmaplot Version 11.2 (Systat Software Inc., CA, USA).

Results

To illustrate the power of "windows of operation", this paper investigated the trade-off between mechanically induced osteogenic differentiation (as measured by COX2 and OPN gene expression levels) and cell detachment in a perfusion-scaffold bioreactor system. Osteoblast-seeded (MC3T3) CG scaffolds having different mean pore sizes (85, 120 and 325μm) were subjected to steady flow regimes with continuous inlet flow-rates of 0 (static), 0.05, 1 and 5mL/min, which equate to mean shear stresses within the scaffold of 0, 0.0009, 0.0176 and 0.0879Pa respectively (McCoy et al., 2012), for a culture period of 48h.

Initially individual contour plots were created for cell detachment (10% intervals) and COX2 (15 fold intervals) gene expression levels across the entire range of scaffold mean pore sizes and mean shear stresses that were included in our evaluation (Figure 1). By specifying required performance limits for the output variables of interest (cell detachment and COX2 gene expression), the acceptable operating ranges for the input variables (mean pore size and shear stress) can be visualised by examining the contour graph. For example, if a cell detachment level of less than 20% is required (light grey in Figure 2a), then at lower mean shear stress levels (<0.03Pa) the scaffold mean pore size should exceed ~100 μm. As the

mean shear stress is increased (>0.03), detachment levels similarly increase at these lower scaffold mean pore sizes and thus an increase in scaffold mean pore size to >~175μm is necessary to maintain the detachment level below 20%. Likewise, to achieve a 60 fold increase in COX2 gene expression (dark grey in Figure 2b), the scaffold mean pore size should be less than 140μm and cells should be exposed to mean shear stresses between 0.25 and 0.65Pa. When individual contour plots are constructed with the same mean pore size and mean shear stress axis ranges, they can be overlaid and the feasible operating ranges for cell detachment and COX2 gene expression can be visualised simultaneously, allowing the user to determine if both performance criteria are achievable at once. For example, when contour plots representing performance criteria of <20% cell detachment and >60 fold increase in COX2 gene expression (Figure 2c) are overlaid, it is clearly seen that there are no operating conditions (mean pore size and shear stress) where both performance criteria can be achieved simultaneously.

Relaxing the user defined constraints in performance criteria for COX2 gene expression to >45 fold increase, yields an enlargement in the potential operating range (Figure 3b). Combining this contour plot with the contour plot representing <20% decrease in cell detachment now yields a single region (black in Figure 3c) on the graph where both operating targets can be achieved simultaneously; a single "window of operation".

If the user defined performance criteria are relaxed further then the feasible operating space, the window of operation (black region in Figure 4), expands accordingly. Relaxation of performance criteria to facilitate a larger feasible operating range may seem illogical as the "optimal" operating conditions are sought. However, so far we have only considered 2 dependent variables, cell detachment and COX2. As additional dependent variables are included in the analysis, it is likely that relaxation of the user defined performance criteria will be necessary in order to obtain a feasible operating region that incorporates all the

dependent variables. For example, the extent of cell differentiation may also be analysed based on the level of OPN gene expression. An individual contour plot representing OPN gene expression levels at 0.4 fold intervals is shown in Figure 5a for the range of mean shear stresses and mean pore sizes investigated in this study. If a performance criteria of greater than 2 fold increase in OPN is set, then it is observed that only a small viable operating range exists for small mean pore sized scaffolds (~<120μm) subjected to the lower range of mean shear stresses (<~0.04Pa) (Figure 5b). If the "optimal" window of operation from Figure 3c is utilized (the feasible operating range for which the highest COX2 gene expression, >45 fold, and lowest cell detachment levels, <20%, could be achieved) and this is overlaid with the feasible operating space for a >2 fold increase in OPN, then there is no "window of operation" in which all three measures of performance can be achieved simultaneously (Figure 5c). However, if we use the feasible operating range studied before (for example, from Figure 4d), where the performance criteria had been relaxed to >15 fold increase in COX2 gene expression and a cell detachment level <40%, we can see that a feasible "window of operation" now exists (cross-hatched area in Figure 5d).

In attempting to manage trade-offs in difference performance criteria it is important to consider the effect of reducing performance limits with respect to all variables. Thus, it may be preferential to sacrifice the level of OPN gene expression with respect to cell detachment and COX2 gene expression. For example, if the performance level for OPN is reduced from a 2 fold increase to a 1.5 fold increase, then in this instance a viable window of operation now comes into existence (cross-hatched area in Figure 6) when using the "optimal" cell detachment/COX2 gene expression performance levels (Figure 3c). Thus a 0.5 fold reduction in OPN gene expression performance level has allowed COX2 gene expression levels to be maintained 30 fold higher and cell detachment levels to be 20% lower.

As the number of measured performance criteria increases, it is obvious to see the power of the "windows of operation" approach in rapidly identifying feasible operating spaces based on user defined requirements for the level of performance. Furthermore, it allows the user to swiftly grasp an understanding of the levels of trade-off between individual performance criteria that may be necessary in order to achieve an "optimal" window of operation.

Discussion

This study illustrates the benefits of a methodology termed "windows of operation" that has previously been employed by the bio-processing community to assist optimisation of large scale protein/antibody manufacture (Salte et al., 2006; Woodley and Titchener-Hooker, 1996; Zhou and Titchener-Hooker, 1999). The "windows of operation" methodology allows visualisation of data to aid decision making by mapping out the feasible operating space for achieving a user-defined level of performance. A simplified perfusion-scaffold bioreactor case study consisting of two independent (scaffold mean pore size and mean shear stress) and three dependent variables (cell detachment, COX2 gene expression and OPN gene expression) was applied to illustrate how this methodology may be applied within the tissue engineering community. Initially using just two of the dependent variables, cell detachment and COX2 gene expression, we illustrated how this tool allowed the rapid identification of feasible operating regions (if they existed) (Figures 2-4) based on the severity of user-defined limitations for the performance criteria. By incorporating a third dependent variable (OPN gene expression) we then demonstrated how this tool could quickly allow the user to examine trade-offs in the performance criteria across multiple variables in order to attain a feasible operating space (Figures 5 and 6).

As previously highlighted this study sought to illustrate how the “windows of operation” tool could be applied within the context of the tissue engineering field. However, it should be noted that prior to such tools being utilised by researchers, the data used must be subjected to a rigorous statistical evaluation and the resulting “window of operation” validated. For example, to generate significantly meaningful contour plots, there must be some degree of covariance between the dependant variable of interest (e.g. cell detachment) and at least one of the independent variables (e.g. mean pore size). If the co-variance between both independent variables (e.g mean pore size and mean shear stress) and the dependent variable is minimal, then in essence the contours could be drawn anywhere through the data set. One potential means to control this is to ensure that the levels of covariance meet a minimum threshold level. However, the magnitude of covariance is not an easily interpretable value as its units are dependent on the variables being studied, but this can be overcome by normalising the covariance to the standard deviations of the data. The resulting value is termed the correlation (a dimensionless number), which always lies on a scale between 1 and -1, where 0 represents no correlation and a negative value implies the variation in the data is inversely related. Strong correlations are considered to exist for data sets having a value between 0.8 and 1 or -0.8 and -1, whilst weak correlations exist between -0.5 and 0.5. In this study, whilst statistical significance within the data was achieved for cell detachment as a function of mean pore size (85 micron vs 325 micron, $P < 0.006$) and for COX2 gene expression as a function of mean shear stress (0.0879Pa vs 0.009Pa, $P < 0.035$), the overall nature of the correlations between the dependent and independent variables ranged from -0.58 and 0.38. This level of general variability within the data, whilst allowing the authors to illustrate how the “windows of operation” may be applied, it is not conducive to subsequent validation of the optimal “windows of operation” described.

In this study we were limited to 2 independent variables (mean pore size and mean shear stress) as the primary focus was to examine trade-offs between multiple dependent variables (cell detachment and measures of cell differentiation). However, for some systems or applications related to tissue engineering there may only be 2 indicators of performance that are of interest, but multiple independent variables that can contribute to changes in these variables. It is important to note therefore that the "windows of operation" tool may also be used in this reverse context, where the user would define operational limits associated with the independent variables to determine what the resulting level of performance would be for the dependent variables. For example, the performance of a process such as tissue decellularization, used in many tissue engineering approaches to provide a starting extracellular matrix for tissue cultivation (Gilbert et al., 2006), may be dependent on the concentration of decellularizing agents reagents (Schaner et al., 2004) or the exposure time of the sample to these agents/procedures, which in essence could be infinite in length. However, often it is desired to complete this process within a set period of time, for example before the extracellular matrix begins to break down and lose its mechanical properties (Sheridan et al., 2012). Thus the user could constrain the operating limits with respect to the independent variables e.g. time, reagent concentrations, temperature etc and examine what the final performance level (decellularization/mechanical properties) would be. The limitations associated with the number of dependent or independent variables studied are reflective of the need to be able to visualise the data graphically. Of course if the user has multiple dependent variables that show a strong positive covariance or more specifically correlation (>0.8), then they may be considered to behave similarly and thus only one of the variables needs be depicted.

In whichever context that "windows of operation" are used, the researcher still needs to conduct the experimental evaluation. The "windows of operation" tool merely models the

existing system, aiding visualisation of the complex data set based on the user defined constraints.

Thus the beneficial application of the information derived from these plots is pre-dominantly associated with two areas; sighting studies or design of experiment (DoE) style experimental set-ups during fundamental research investigations and process development decision making for products pre-commercialisation.

For DoE style studies or sighting studies, researchers at early investigatory stages may have an extensive range for a parameter that they wish to study. Application of "windows of operation" may help narrow down future operating ranges so that more subtle differences in performance criteria can be examined. For example in this study, the shear stress range initially studied was between 0 and ~0.1Pa, having applied "windows of operation", future studies may now be conducted between 0.04 and 0.08Pa range (Figure 6), as this is the optimal zone for the performance criteria evaluated (COX2 gene expression, OPN gene expression and cell detachment) based on the trade-offs made between these performance criteria.

In terms of process development decision making, in paradigms such as tissue engineering, the biological product (the tissue) is defined by the respective manufacturing process and hence the product and process cannot be considered independently of each other – as shown in this study. This is an important fact to consider as the tissue engineering field matures and researchers shift their focus from fundamental research towards clinical application of the developed tissues. Whilst clinical success is by no doubt the single biggest factor for a new product, current regulatory and industrial thinking also requires product quality to be designed into the manufacturing process; through a systematic development programme generally termed ''Quality by Design" (Q8 ICH Draft Guidance on Pharmaceutical Development). To undertake this successfully, it is important to begin considering its

relevance at early stages of the development programme. These process-dependent programmes are concerned with controlling the manufacturing conditions to ensure tissues of an expected quality are delivered. They are typically based on risk analysis approaches founded on the knowledge-design-control concept. In this concept, the knowledge space represents the broader understanding of the relationship between the process operation and product quality, the design space represents the established range of process parameters that have been demonstrated to yield an assurance of quality (a specific level of performance) and the control space is a constrained set of tighter operating conditions within the design space. "Windows of operation" tools applied to the comprehensive data sets generated during the research stages of the project, provide a simple way of embodying the first two levels of this philosophy (Figure 7), where the total area of the plot generated would be representative of the knowledge space, and the window of operation or feasible operating space is then representative of the design space. Having established a feasible operating space, the researcher then needs to determine where the control space should be located within this design space. If the feasible operating space is small in nature or tightly constrained, then there may be a limited choice. However, if the operating space is large in nature, such as in Figure 4d or if there are multiple feasible operating spaces, as shown in a hypothetical window of operation diagram in Figure 8, then in these instances other factors such as economics or time may contribute to the decisions made regarding allocation of the control space. For example in the context of the current study, to fabricate 85μm mean pore size scaffolds, more power and longer freeze-dryer running cycles are needed in comparison to 325μm scaffolds, leading to higher electricity bills. Thus in the instance of the hypothetical window in Figure 8, where scientific evaluation has determined that multiple feasible operating windows exist, it may be a business decision that drives location of the control space.

In summary, in this study we have shown how “windows of operation” may be employed by the tissue engineering community using a perfusion-scaffold bioreactor system as a case study. Incorporation of such tools into the tissue engineer’s armoury will hopefully yield a greater understanding of the highly complex systems used and help aid decision making in future translation of products from the bench top to the market place.

Acknowledgements

This study has received funding from the European Research Council under the European Community's Seventh Framework Programme (FP7/2007-2013) / ERC grant agreement n° 239685. Collagen materials were provided by Integra Life Sciences, Inc. through a Material Transfer Agreement.

References

Alvarez-Barreto JF, Sikavitsas VI. 2007. Improved mesenchymal stem cell seeding on RGD modified poly(L-lactic acid) scaffolds using flow perfusion. Macromolecular Bioscience 7:579-588.

Alvarez-Barreto J, Linehan S, Shambaugh R, Sikavitsas V. 2007. Flow perfusion improves seeding of tissue engineering scaffolds with different architectures. Annals of Biomedical Engineering 35:429-442.

Annaz B, Hing KA, Kayser M, Buckland T, Silvio LD. 2004. Porosity variation in hydroxyapatite and osteoblast morphology: a scanning electron microscopy study. Journal of Microscopy 215:100-110.

Cartmell, S., Porter, B.D, García, A.J., Guldberg, R.E. 2003. Effects of medium perfusion rate on cell-seeded three-dimensional bone constructs in vitro. Tissue Engineering 9:1197.

Forwood MR. 1996. Inducible cyclo-oxygenase (COX-2) mediates the induction of bone formation by mechanical loading in vivo. Journal of Bone and Mineral Research 11:1688-1693.

Gilbert TW, Sellaro TL, Badylak SF. 2006. Decellularization of tissues and organs. Biomaterials 27:3675-3683.

Jaasma MJ, O'Brien FJ. 2008. Mechanical stimulation of osteoblasts using steady and dynamic fluid flow. Tissue Eng Part A 14:1213-1223.

Jungreuthmayer C, Jaasma MJ, Al-Munajjed AA, Zanghellini J, Kelly DJ, O'Brien FJ. 2009. Deformation simulation of cells seeded on a collagen-GAG scaffold in a flow perfusion bioreactor using a sequential 3D CFD-elastostatics model. Medical Engineering & Physics 31:420-427.

Keogh MB, Partap S, Daly JS, O'Brien FJ. 2011. Three hours of perfusion culture prior to 28 days of static culture, enhances osteogenesis by human cells in a collagen GAG scaffold. Biotechnol. Bioeng 108:1203-1210.

Klein-Nulend J, Burger EH, Semeins CM, Raisz LG, Pilbeam CC. 1997. Pulsating Fluid Flow Stimulates Prostaglandin Release and Inducible Prostaglandin G/H Synthase mRNA Expression in Primary Mouse Bone Cells. Journal of Bone and Mineral Research 12:45-51.

Langer R, Vacanti J. 1993. Tissue engineering. Science 260:920 -926.

Livak KJ, Schmittgen TD. 2001. Analysis of Relative Gene Expression Data Using Real-Time Quantitative PCR and the 2-[Delta][Delta]CT Method. Methods 25:402-408.

McCoy RJ, Jungreuthmayer C, O'Brien FJ. 2012. Influence of flow-rate and scaffold pore size on cell behaviour during mechanical stimulation in a flow perfusion bioreactor. Biotechnology and Bioengineering. In print: DOI: 10.1002/bit.24424.

McMahon L. 2007. The effect of cylic tensile loading and growth factors on the chondrogenic differentiation of bone-marrow derived mesenchymal stem cells in a collagen-glycosaminoglycan scaffold. PhD Thesis, Trinity College Dublin, Dublin.

Murphy CM, Haugh MG, O'Brien FJ. 2010. The effect of mean pore size on cell attachment, proliferation and migration in collagen-glycosaminoglycan scaffolds for bone tissue engineering. Biomaterials 31:461-466.

O'Brien FJ, Harley BA, Yannas IV, Gibson LJ. 2005. The effect of pore size on cell adhesion in collagen-GAG scaffolds. Biomaterials 26:433-441.

O'Brien FJ, Harley BA, Yannas IV, Gibson L. 2004. Influence of freezing rate on pore structure in freeze-dried collagen-GAG scaffolds. Biomaterials 25:1077-1086.

Partap S, Plunkett N, Kelly DJ, O'Brien FJ. 2009. Stimulation of osteoblasts using rest periods during bioreactor culture on collagen-glycosaminoglycan scaffolds. J Mater Sci: Mater Med 21:2325-2330.

Plunkett NA, Partap S, O'Brien FJ. 2010. Osteoblast response to rest periods during bioreactor culture of collagen-glycosaminoglycan scaffolds. Tissue Eng Part A 16:943-951.

Salte H, King JMP, Baganz F, Hoare M, Titchener-Hooker NJ. 2006. A methodology for centrifuge selection for the separation of high solids density cell broths by visualisation of performance using "windows of operation". Biotechnology and Bioengineering 95:1218-1227.

Schaner PJ, Martin ND, Tulenko TN, Shapiro IM, Tarola NA, Leichter RF, Carabasi RA, DiMuzio PJ. 2004. Decellularized vein as a potential scaffold for vascular tissue engineering. Journal of Vascular Surgery 40:146-153.

Sheridan WS, Duffy GP, Murphy BP. 2012. Mechanical characterization of a customized decellularized scaffold for vascular tissue engineering. Journal of the Mechanical Behavior of Biomedical Materials 8:58-70.

Wadhwa S, Choudhary S, Voznesensky M, Epstein M, Raisz L, Pilbeam C. 2002a. Fluid flow induces COX-2 expression in MC3T3-E1 osteoblasts via a PKA signaling pathway. Biochemical and Biophysical Research Communications 297:46-51.

Wadhwa S, Godwin SL, Peterson DR, Epstein MA, Raisz LG, Pilbeam CC. 2002b. Fluid Flow Induction of Cyclo-Oxygenase 2 Gene Expression in Osteoblasts Is Dependent on an Extracellular Signal-Regulated Kinase Signaling Pathway. Journal of Bone and Mineral Research 17:266-274.

Woodley JM, Titchener-Hooker NJ. 1996. The use of windows of operation as a bioprocess design tool. Bioprocess Engineering 14:263-268.

Zhang X, Schwarz EM, Young DA, Puzas JE, Rosier RN, O'Keefe RJ. 2002. Cyclooxygenase-2 regulates mesenchymal cell differentiation into the osteoblast lineage and is critically involved in bone repair. J Clin Invest 109:1405-1415.

Zhou YH, Titchener-Hooker NJ. 1999. Visualizing integrated bioprocess designs through "windows of operation." Biotechnology and Bioengineering 65:550-557.

Figure Legends

Figure 1: Contour plot representations of (A) cell detachment and (B) fold change in COX2 gene expression levels for osteoblast cell-seeded scaffolds having a range of mean pore sizes (85, 120 or 325 μm) after being subjected to various levels of mean shear stress (0.0009, 0.0176 and 0.0879Pa) for 48h in a perfusion bioreactor. Cell detachment contour lines represent the percentage of cells detached and are spaced at 10% intervals. COX2 gene expression contours represent fold change in comparison to static controls at 0h and are spaced at 15 fold intervals.

Figure 2: Creating a "window of operation". Based on user-defined performance levels for (A) cell detachment (<20%) and (B) COX2 gene expression (>60 fold increase), contour plots illustrating the operating regions in which these can be achieved are displayed either individually (A+B) or combined (C). Combining contour plots allows rapid and easy visualisation of operational areas where the user-defined performance levels for both outputs can be achieved simultaneously. In this instance (C) there is no region on the graph where both operating targets can be achieved simultaneously i.e no "window of operation".

Figure 3: Creating a "window of operation". Based on user-defined performance levels for (A) cell detachment (<20%) and (B) COX2 gene expression (>45 fold increase), contour plots illustrating the operating regions in which these can be achieved are displayed individually (A+B) or combined (C). Combining contour plots allows rapid and easy visualisation of operational areas where the user-defined requirements for both outputs can be achieved. In this instance there is a single region (black) on the graph (C) where both operating targets can be achieved simultaneously; a single "window of operation".

Figure 4: Assessing changes in the feasible operation space as a function of changes in user-defined performance criteria. (A) The initial window of operation (black) based on the user-defined specifications for cell detachment of <20% (light grey) and COX2 gene expression (dark grey) of >45 fold increase. (B) Relaxation of the performance level for cell detachment to <25%. (C) Relaxation of the performance level for cell detachment to <25% and for COX2 gene expression levels to >25 fold increase. (D) Relaxation of the performance levels for cell detachment to <40% and for COX2 gene expression levels to >15 fold increase. As the performance levels are relaxed, changes in the size and shape of the window of operation (black) leading to larger feasible operating ranges are clearly visible.

Figure 5: Effect of a 3rd measure of performance (OPN gene expression level) on the feasible operating space. (A) Contour plot showing changes in OPN gene expression level compared to 0h control. (B) Feasible operating space (grey) for a performance level representative of >2fold increase in OPN gene expression level. (C) Based on the "optimal" window of operation for cell detachment and COX2 gene expression (Figure 4a) no feasible window of operation exists where all three performance criteria can be achieved. (D) Relaxation of cell detachment and COX2 gene expression performance criteria to the levels in Figure 4d yields a small feasible window of operation (cross-hatched) where all three performance criteria can be achieved.

Figure 6: Evaluating trade-offs in performance criteria. Figure 5 highlighted how large sacrifices in user-defined performance criteria for COX2 gene expression and cell detachment were necessary in order to find a viable operating space that also included the required performance level (>2 fold) for OPN. Alternatively, a small sacrifice in OPN gene

expression to >1.5 yields a result where all three performance criteria (cross-hatched) can be achieved within the original “optimal” window of operation for COX2 gene expression and cell detachment.

Figure 7: Knowledge-Design-Control space paradigm. On the left is a diagrammatic representation of the Knowledge-Design-Control space paradigm, where the knowledge space represents the broader understanding of the relationship between the process operation and product quality, the design space represents the established range of process parameters that have been demonstrated to yield an assurance of quality (a specific level of performance) and the control space is a constrained set of tighter operating conditions within the design space. “Windows of operation” tools, as depicted on the right, provide a simple way of embodying the first two levels of this philosophy, where the total area of the plot generated is representative of the knowledge space and the window of operation or feasible operating space is then representative of the design space.

Figure 8: Hypothetical contour plot having two feasible windows of operation (black).

Figures

Figure 1

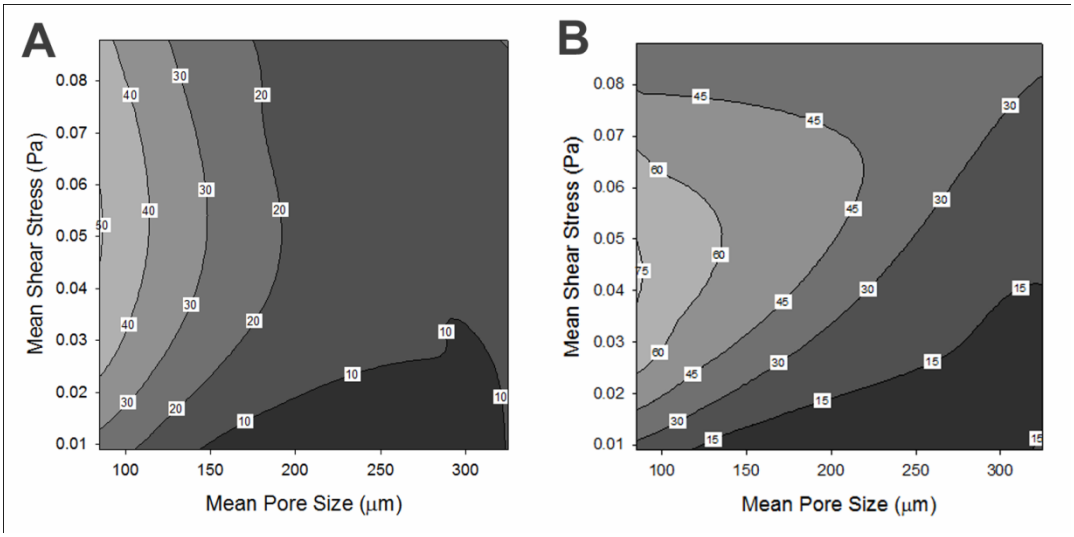

Figure 2

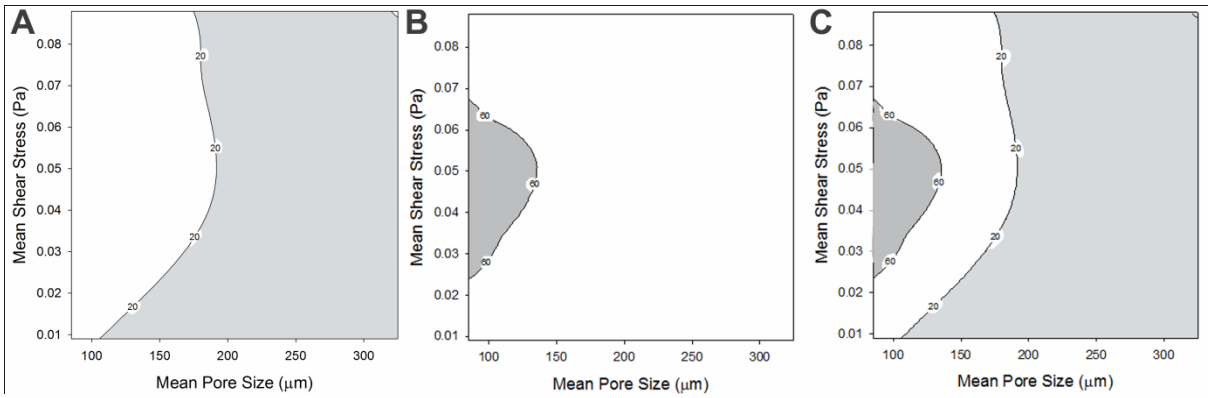
A
B
C
Mean Shear Stress (Pa)
0.08
0.07
0.06
0.05
0.04
0.03
0.02
0.01
100
150
200
250
300
Mean Pore Size (μm)
20
60

Figure 3

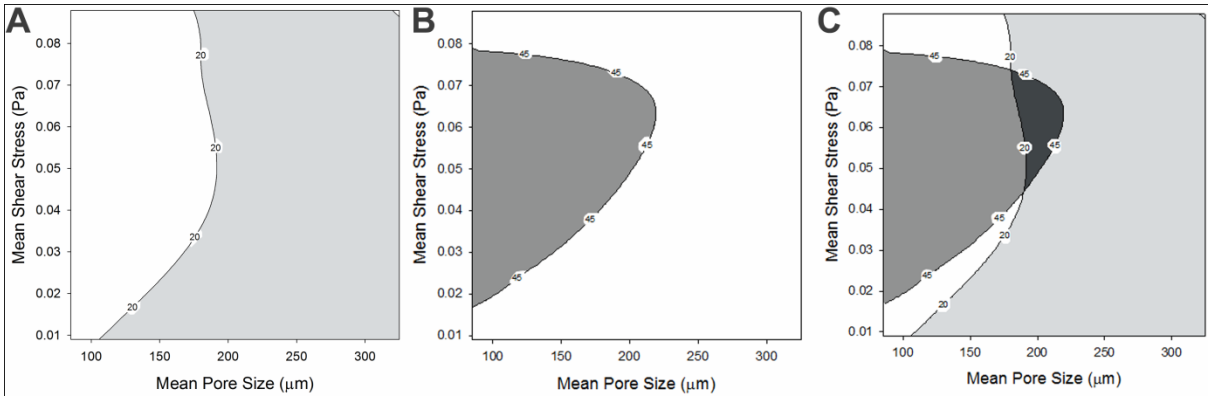
A
B
C
Mean Shear Stress (Pa)
0.08
0.07
0.06
0.05
0.04
0.03
0.02
0.01
100
150
200
250
300
Mean Pore Size (μm)
20
45

Figure 4

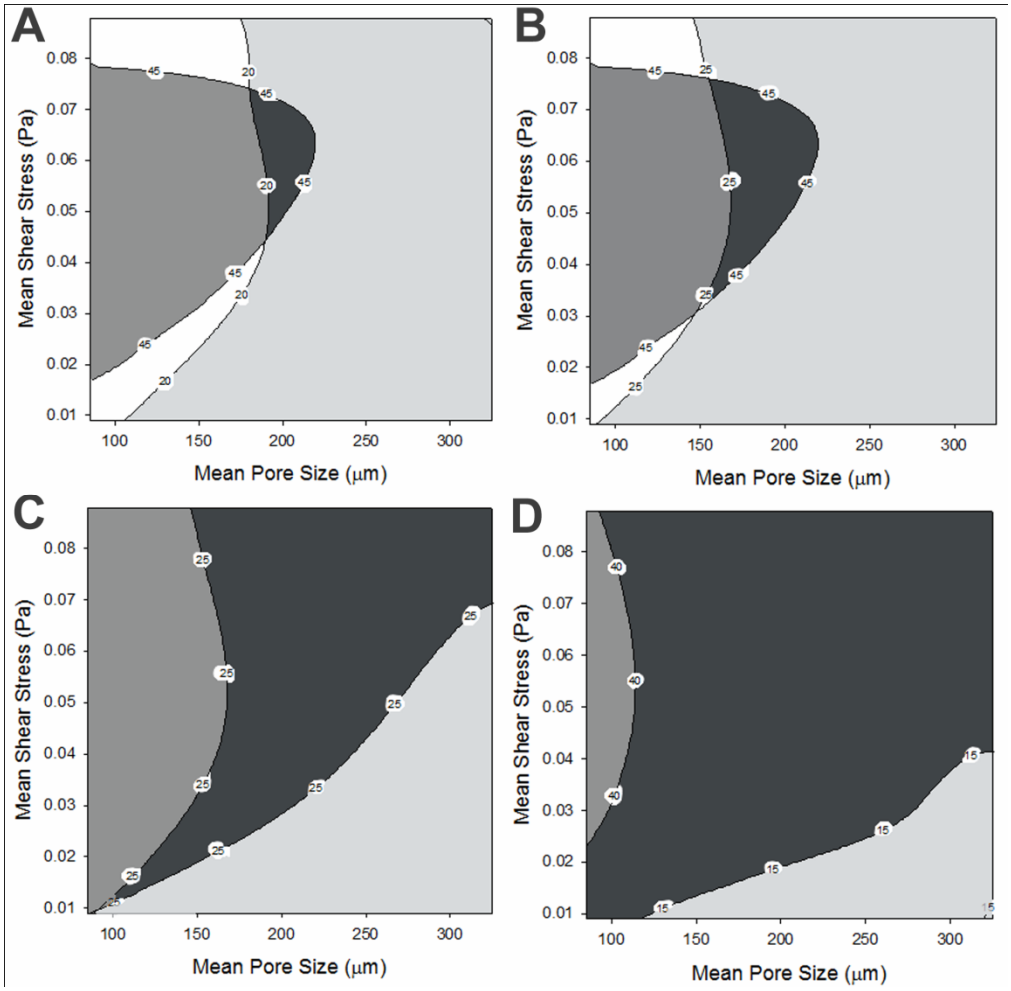
A
B
C
D
Mean Shear Stress (Pa)
Mean Pore Size (μm)
0.01
0.02
0.03
0.04
0.05
0.06
0.07
0.08
100
150
200
250
300
45
20
25
40
15

Figure 5

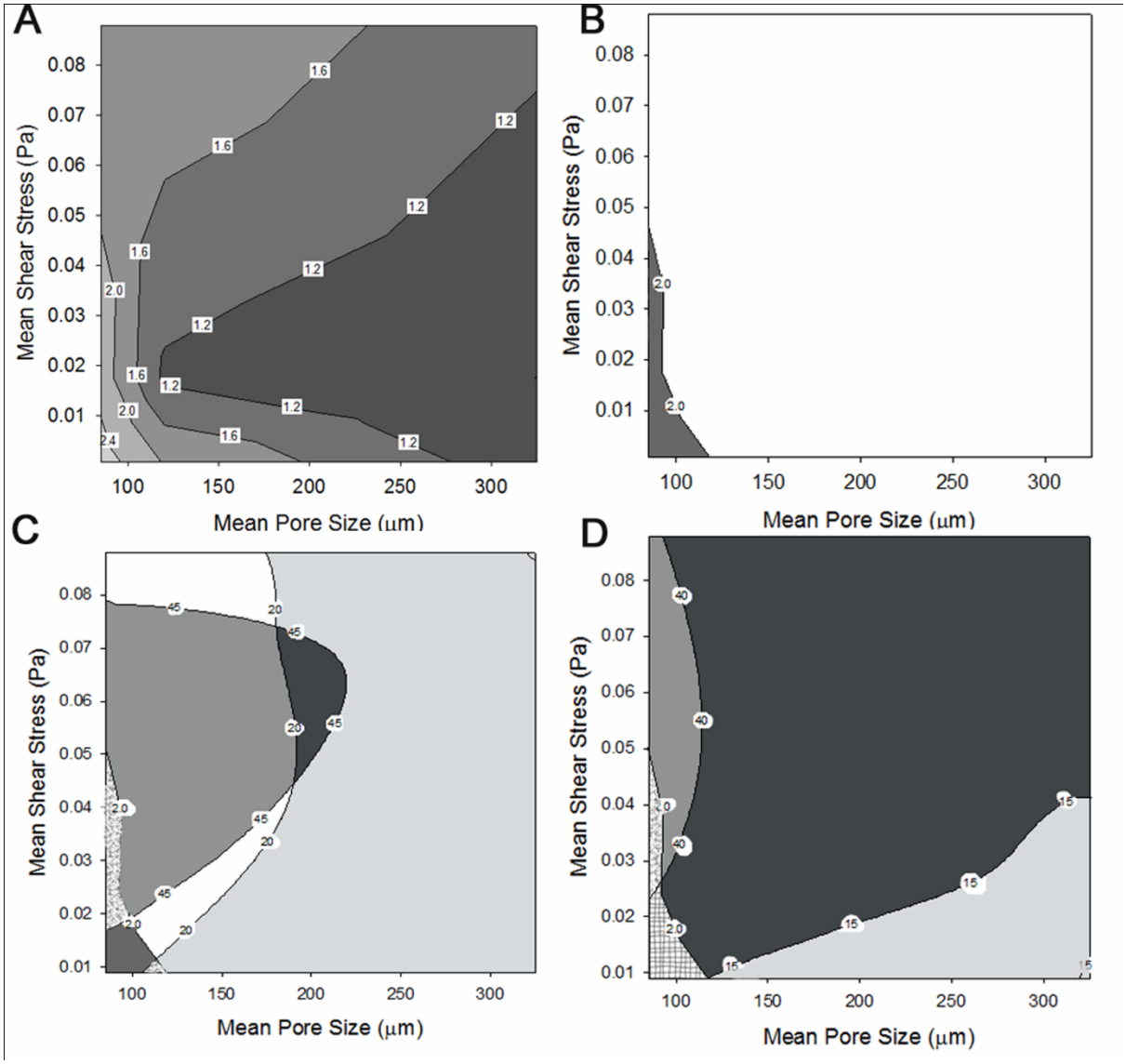
A
B
C
D
Mean Shear Stress (Pa)
Mean Pore Size (μm)
0.08
0.07
0.06
0.05
0.04
0.03
0.02
0.01
100
150
200
250
300
1.6
1.2
2.0
2.4
45
20
40
15

Figure 6

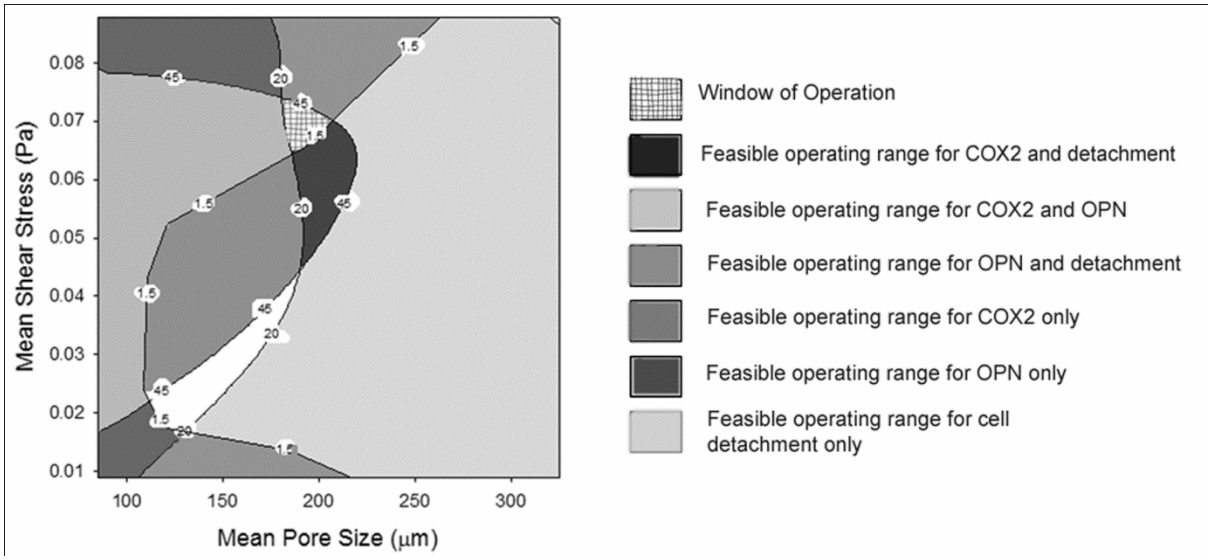

Figure 7

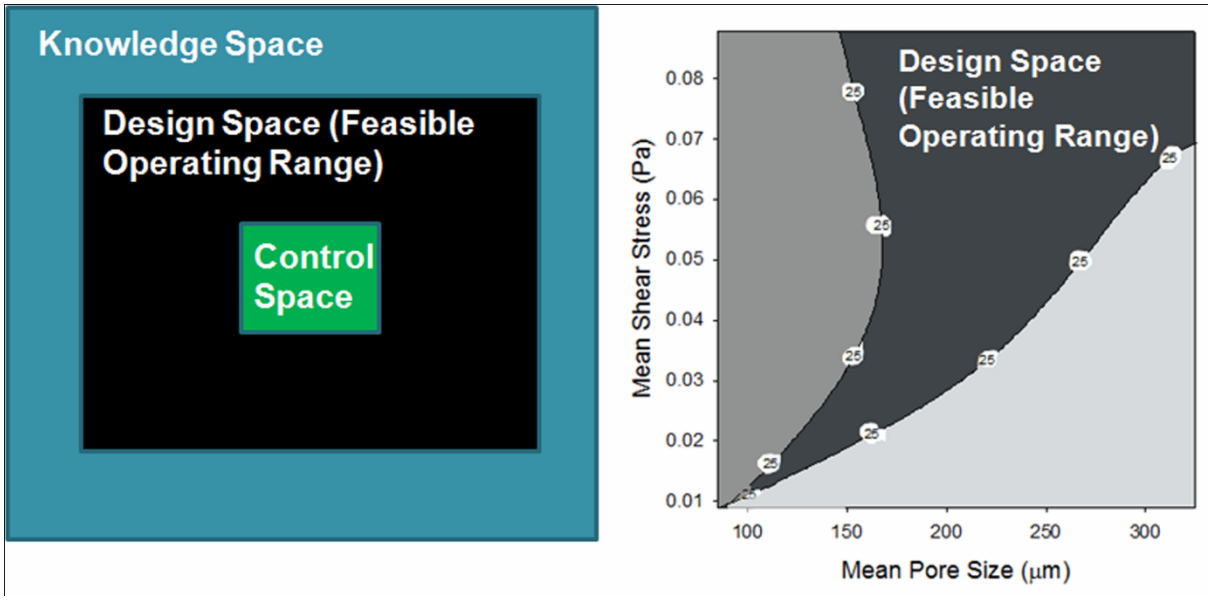

Figure 8

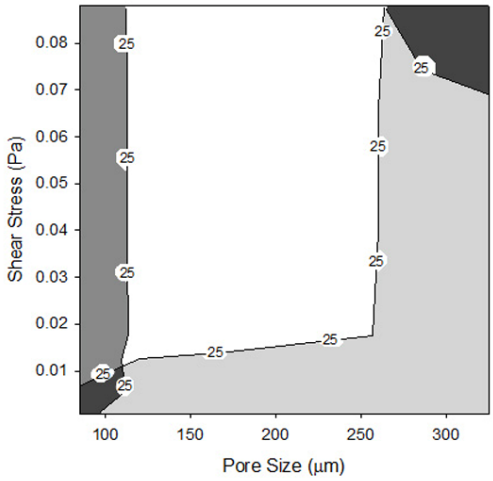
Shear Stress (Pa)
0.08
0.07
0.06
0.05
0.04
0.03
0.02
0.01
100
150
200
250
300
Pore Size (µm)
25